Published for SISSA by Springer

Received: *September 9, 2014*
Accepted: *November 3, 2014*
Published: *November 17, 2014*

Top-quark mass effects in double and triple Higgs production in gluon-gluon fusion at NLO

F. Maltoni,[a] **E. Vryonidou**[a] **and M. Zaro**[b]

[a] *Centre for Cosmology, Particle Physics and Phenomenology (CP3), Université Catholique de Louvain, B-1348 Louvain-la-Neuve, Belgium*

[b] *Sorbonne Universités, UPMC Univ. Paris 06, UMR 7589, LPTHE, and CNRS, UMR 7589, LPTHE, F-75005, Paris, France*

E-mail: fabio.maltoni@uclouvain.be, evryonidou@gmail.com, marco.zaro@lpthe.jussieu.fr

Abstract: The observation of double and triple scalar boson production at hadron colliders could provide key information on the Higgs self couplings and the potential. As for single Higgs production the largest rates for multiple Higgs production come from gluon-gluon fusion processes mediated by a top-quark loop. However, at variance with single Higgs production, top-quark mass and width effects from the loops cannot be neglected. Computations including the exact top-quark mass dependence are only available at the leading order, and currently predictions at higher orders are obtained by means of approximations based on the Higgs-gluon effective field theory (HEFT). In this work we present a reweighting technique that, starting from events obtained via the MC@NLO method in the HEFT, allows to exactly include the top-quark mass and width effects coming from one- and two-loop amplitudes. We describe our approach and apply it to double Higgs production at NLO in QCD, computing the needed one-loop amplitudes and using approximations for the unknown two-loop ones. The results are compared to other approaches used in the literature, arguing that they provide more accurate predictions for distributions and for total rates as well. As a novel application of our procedure we present predictions at NLO in QCD for triple Higgs production at hadron colliders.

Keywords: Higgs Physics, QCD, Standard Model

ArXiv ePrint: 1408.6542

doi:10.1007/JHEP11(2014)079

JHEP11(2014)079

Contents

JHEP11(2014)079

1 Introduction

Present LHC data already provide convincing evidence that the scalar particle observed at the LHC is the one predicted by the Brout-Englert-Higgs breaking mechanism [1, 2] of the $SU(2)_L \times U(1)_Y$ symmetry as implemented in the Standard Model (SM) [3]. Here, the strength of the Higgs boson couplings is uniquely determined by the masses of the elementary particles, including the Higgs boson itself. The measured couplings to fermions and vector bosons are found to agree within 10–20% with the SM predictions [4–11]. No direct information, however, has been collected so far on the Higgs self-couplings that appear in the potential:

$$V(H) = \frac{1}{2}m_H^2 H^2 + \lambda_{HHH} v H^3 + \frac{1}{4}\lambda_{HHHH} H^4. \tag{1.1}$$

The values of the Higgs self-couplings λ_{HHH} and λ_{HHHH} are fixed in the SM by gauge invariance and renormalisability to $\lambda_{HHH} = \lambda_{HHHH} = m_H^2/2v^2$, i.e. fully determined by the mass of the Higgs boson and the Higgs field vacuum expectation value v. Direct information on the Higgs three-point and four-point interactions would therefore provide key information on the upper scale of validity of the SM when thought of as an effective theory itself, or on the possible existence of a richer scalar sector, featuring additional scalar fields, possibly in other representations.

In this context, multiple Higgs production plays a special role. At the lowest order, Higgs pair production is the simplest production process that is sensitive to the trilinear self-coupling λ_{HHH}, while to probe the quartic Higgs coupling λ_{HHHH} one would need to consider at least triple Higgs production. Unfortunately, in the SM multiple Higgs production rates at the LHC are quite small [12, 13] and the prospects of making precise enough measurements at the LHC (assuming SM values) are at best challenging [14–16] for double Higgs production and rather bleak for triple Higgs production [13, 17].

However, multiple Higgs production rates could be enhanced by new physics effects and therefore the process provides one with a wealth of possibilities for probing new physics. These possibilities range from explicit models featuring new particles, such as the 2HDM [18–21], SUSY [12, 22–24], extended colored sectors [25–27], Little Higgs Models [28, 29], Higgs portal [30, 31], flavor symmetry models [32] and Composite Higgs models [33, 34] to model independent higher-dimensional interactions [35–37]. In any case, precise predictions for rates and distributions will be needed to be able to extract valuable information on λ_{HHH} or on new physics effects in general. Higgs pair production will be relevant for the high-luminosity LHC and several phenomenological studies [38–47] have recently investigated the potential of detecting the signal for the process over the backgrounds in various Higgs decay channels. Triple Higgs production rates are smaller by more than two orders of magnitude [13, 17], making the process possibly relevant for a future 100 TeV collider.

Analogously to single Higgs production, several channels can lead to a final state involving two or three Higgs bosons. They involve either the Higgs coupling to the top quark (e.g., gluon-gluon fusion via top loops and $t\bar{t}$ associated production), or to vector bosons (e.g., vector boson fusion and associated production), or to both (e.g., single-top associated production). The dominant production mechanism for multiple Higgs production is gluon-gluon fusion via top-quark loops, exactly as in the case of single Higgs production. Cross sections corresponding to the other channels are at least one order of magnitude smaller, even though possibly interesting because of different sensitivity to the λ's or to other couplings, such as $VVHH$ [48, 49], or to new physics. In addition, typically, different channels open different possibilities of exploiting a wider range of Higgs decay signatures. Predictions for the six main HH production channels at NLO in QCD for hadron collider energies ranging from 8 to 100 TeV can be found in [50]. NNLO results for vector boson fusion [51] and vector boson associated production [39] are also available. For triple Higgs production gluon-gluon fusion is again the dominant production channel by at least one order of magnitude. However, the importance of the subdominant production channels is slightly different from the pair production at 14 TeV, with $t\bar{t}$ associated production giving the second largest contribution, and VBF the third.

Gluon-gluon fusion being the dominant production mechanism for multiple Higgs-boson production, one would like to have the most accurate and precise predictions possible for this channel. However, as Higgs pair production is a loop induced $2 \to 2$ process at the Born level, higher-order computations become very involved. Computations including the exact top-quark mass dependence, i.e. in the Full Theory (FT), are only available at the leading order, and currently predictions at NLO [52] and NNLO accuracy [53, 54] are obtained by means of approximations that build upon the Higgs-gluon effective field theory. Besides, at variance with the inclusive cross section computation for single Higgs production, top-quark mass effects in the loops cannot be neglected. In this work we present a method that, starting from an NLO calculation matched to parton shower (PS) in the Higgs effective-field theory allows us to systematically include the heavy-quark mass effects coming from the one- and two-loop amplitudes, as long as results for the latter are available. We describe our approach, validate it against single Higgs production, for

JHEP11(2014)079

which all the necessary loop amplitudes are known, and apply it to double and triple Higgs production using all available information, i.e. the exact one-loop (real) amplitudes and the known parts of the two-loop amplitudes. We dub our results $\text{FT}_{\text{approx}}$ at NLO(+PS) and compare them to other approximations in the literature. We show that with just the currently available information on the loop amplitudes, our reweighting method already provides more accurate results for the differential distributions at NLO plus parton shower level and argue that that is the case for total rates as well.

The paper is structured as follows. In section 2 we discuss the current status of the computation for multiple Higgs production. In section 3 we describe our method and in particular how the top-quark mass effects can be consistently included in the calculation. In section 4 we present our results for Higgs pair production, comparing our method with previous results in the literature. In section 5 for the first time we present results for triple Higgs production beyond the leading order, obtained using the same method. We summarise our findings and draw some conclusions in the final section.

2 Multiple Higgs production in gluon-gluon fusion

In this section we briefly summarise the state-of-the-art in the computation of multiple Higgs production in gluon-gluon fusion. For the sake of conciseness we will focus only on Higgs pair production, most of the features being easily extendable to the general case. In the SM, the diagrams contributing to the gluon-gluon fusion channel can be organised in two classes: those where both Higgs bosons couple to the heavy quarks in the loop and those that feature the Higgs self coupling. The corresponding classes of diagrams appearing at the leading order are shown in figure 1. At NLO, $2 \to 3$ real one-loop diagrams, figure 2 a), and $2 \to 2$ virtual two-loop diagrams, both boxes and triangles, figure 2 b), contribute, each of them being infrared divergent yet overall giving a finite result when combined in the computation of collinear and infrared safe observables. The one-loop matrix elements entering the Born amplitude as well as the real corrections can be obtained using modern loop techniques [55] automatically [56]. The two-loop triangles (such as the first one in figure 2 b)) featuring the Higgs self coupling are the same as those entering the single Higgs production and therefore also known for a long time [57–59] and used in publicly available codes for single Higgs production [60, 61]. The two-loop box amplitudes, however, are not known. This computation is extremely challenging due to the presence of several scales (s, t, u, m_H^2, m_t^2) in the loops and is currently out of reach. As it will become clear in the coming section, our reweighting technique can efficiently provide the NLO result with the full top-quark mass dependence once the corresponding amplitudes become known.

In the meantime, precisely due to the difficulty of including higher-order corrections exactly, the strategy widely employed for single Higgs-boson production has been adopted for Higgs pair production. An effective field theory, where the top quark has been integrated out from the theory and the Higgs boson couples directly to the gluon field, has been introduced, where the corresponding lagrangian reads

$$\mathcal{L}_{\text{HEFT}} = \frac{\alpha_S}{12\pi} G^a_{\mu\nu} G^{a,\mu\nu} \log\left(1 + \frac{H}{v}\right), \tag{2.1}$$

JHEP11(2014)079

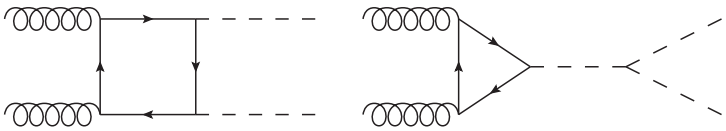

Figure 1. Representative Feynman diagrams for box and triangle topologies for Higgs pair production in gluon-gluon fusion at the lowest order in perturbative QCD. The two gauge-indepedent classes of diagrams interfere destructively.

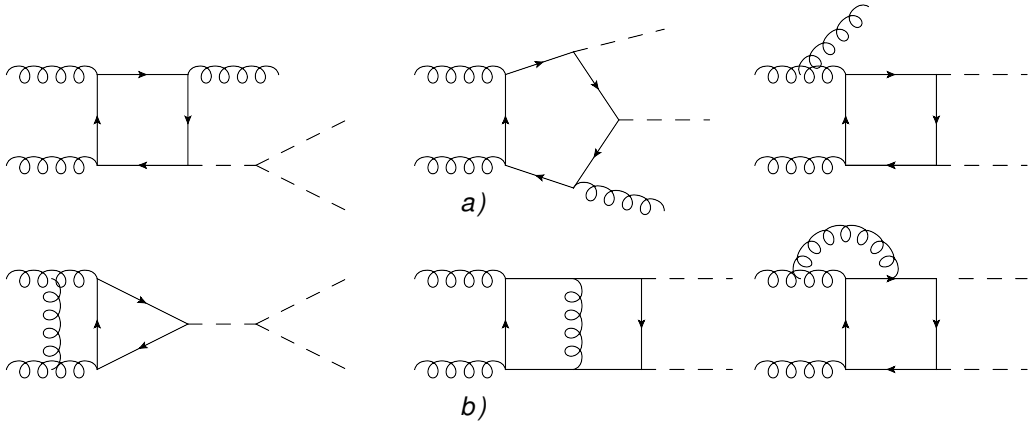

Figure 2. Sample of Feynman diagrams for the NLO Higgs pair production in gluon-gluon fusion. a) Real one-loop and b) virtual two-loop corrections.

G being the QCD field tensor. The main motivation for using this approximation is that it makes the computation of higher-order corrections feasible. The approximation has been proven to work extremely well for single Higgs production [62]. The HEFT provides accurate predictions for the total rates as well as for the differential distributions when the invariants involved are not much larger than the top quark mass. Unfortunately, in the case of double Higgs production, the relevant scale is at least the invariant mass of the HH pair which is typically $\gtrsim 2m_t$ and therefore the HEFT provides only a rough approximation for the total rates and a very poor one for the relevant distributions [25, 40].

Given the fact that the full NLO results are not presently available and that the HEFT gives a poor description of the process, efforts have been made to improve results taking into account heavy-quark loop effects at least in an approximated way. A first step in this direction has been taken in the seminal NLO calculation for Higgs pair production, as implemented in the code HPAIR [12, 52], which provides total cross sections in the SM and in SUSY. In this case, the NLO calculation is performed within the HEFT, yet all contributions (virtual and real) to the short-distance parton-parton cross section are expressed in terms of the LO cross section times an α_S correction. The LO cross section in the HEFT is then substituted by the LO one with the full heavy-quark mass dependence. As the aim of HPAIR is to provide results for the total cross section, this approximation is certainly a first useful step. However, such an approach is obviously not suitable in general and in particular for observables that receive considerable contributions from the real $2 \to 3$

JHEP11(2014)079

configurations, the most glaring example being the tail of the transverse momentum of the Higgs pair, $p_T(HH)$.

We also mention that the top-quark mass effects at NLO in QCD have been estimated through an $1/m_t^2$ expansion [63] (on which we will further comment later). The NNLO computation for total rates in the HEFT [53] has also now been completed with the calculation of the three-loop matching coefficient C_{HH} [54], while recently results have been obtained by merging samples of different parton multiplicities in [43, 64] and including threshold resummation [65].

3 The inclusion of heavy-quark loop effects

In this section we discuss how to improve further on the HEFT approximation, and in particular how one can improve on pure NLO in HEFT by including heavy-quark loop effects in the Born amplitude as well as in the real emission ones. Results using this method have already been presented in [50]. They have been achieved by implementing all the ingredients in an automatically generated code for the HEFT within the MadGraph5_aMC@NLO framework [66]. In practice, the effective Lagrangian of eq. (2.1) is implemented in FeynRules [67, 68][1] upgraded to NLO by including the necessary UV and R_2 counter terms [55, 72–75] to obtain a UFO model [76, 77] that can be imported in MadGraph5_aMC@NLO. At this point NLO parton-level events can be automatically generated in the HEFT and then reweighted on an event-by-event basis using the appropriate heavy-quark loop amplitudes.

To include the heavy-quark amplitudes we make use of the structure of an NLO calculation as performed within MadGraph5_aMC@NLO. For completeness, let us consider the computation of a cross section at NLO, namely

$$d\sigma = d\phi_n \left(\mathcal{B} + \mathcal{V} + \mathcal{C}^{\text{int}}\right) + d\phi_{n+1} \left(\mathcal{R} - \mathcal{C}\right) , \tag{3.1}$$

where $\mathcal{B}, \mathcal{V}, \mathcal{R}$ are respectively the Born, virtual and real emission contributions, $\mathcal{C}$ are the local counterterms (needed in order to render the integral over $d\phi_{n+1}$ finite) and $\mathcal{C}^{\text{int}}$ is the integrated form of $\mathcal{C}$ (over the extra parton phase space). The detailed form of the counterterms $\mathcal{C}^{(\text{int})}$ depends on the subtraction scheme in use for the computation (e.g., FKS [78] or CS [79]). In general they involve a Born matrix element times some process-independent splitting kernel together with a dedicated phase-space mapping.

A very similar formulation as the one above holds in the case of matching NLO computations with parton-shower in the MC@NLO formalism, where on top of the local counterterms $\mathcal{C}$ one has to also include the so-called Monte-Carlo counterterms $\mathcal{C}_{\text{MC}}$ [80]. The important difference with respect to the NLO formulation of eq. (3.1) is that the MC counterterms are such that Born-like ($\mathbb{S}$-events) and real-emission ($\mathbb{H}$-events) unweighted events can obtained as the corresponding subtracted cross sections are separately finite.

[1] More complete implementations including interactions coming from the full set of dimension-six operators are also available [69–72].

JHEP11(2014)079

The corresponding contributions to the total cross section can be written as

$$d\sigma^{(\mathbb{H})} = d\phi_{n+1}\left(\mathcal{R} - \mathcal{C}_{\rm MC}\right) , \tag{3.2}$$

$$d\sigma^{(\mathbb{S})} = d\phi_{n+1}\left[\left(\mathcal{B} + \mathcal{V} + \mathcal{C}^{\rm int}\right)\frac{d\phi_n}{d\phi_{n+1}} + \left(\mathcal{C}_{\rm MC} - \mathcal{C}\right)\right] . \tag{3.3}$$

In the MadGraph5_aMC@NLO framework, one can automatically generate the code corresponding to the Born, virtual, real amplitudes, the counter terms and the phase space [56, 81] in one go in order to compute cross sections and generate events for $gg \to HH$ at NLO in QCD in the HEFT. All the finite heavy-quark one-loop matrix-elements (i.e. those entering the Born and real contributions) needed can also be obtained within MadGraph5_aMC@NLO. Note, however, that two limitations presently make the *automatic* computation of the exact NLO result not possible. First, the computation of cross sections that have a loop Born matrix-element is not automated yet (even at the LO only). Second, even with the automation for loop-induced processes, the need for the two-loop amplitudes would require an external routine, as this cannot be performed automatically by MadLoop. Therefore, the inclusion of heavy-quark effects needs manipulation that can in principle be performed in two ways.

The first option is to generate the code for an NLO computation in the HEFT and then replace the matrix-elements (for $\mathcal{B}, \mathcal{V}, \mathcal{R}, \mathcal{C}^{\rm int}$ and $\mathcal{C}_{\rm MC}$) with the corresponding ones in the FT. Even though this is the simplest option, it features several drawbacks. First, this method is very inefficient as the (computationally expensive) one-loop and two-loop matrix elements routines would then be called many times to probe and map all regions of phase space. In addition, it requires the evaluation of the real one-loop matrix elements in the FT in regions of phase space very close to the soft/collinear limits, i.e. where they might feature unstable configurations. For such points, multiple precision needs to be employed at the cost of a growth of the running time by a factor of a hundred.

The second option is to include the top-quark mass effects by reweighting after having generated the short-distance events and before these are passed to a parton shower program. In order for this procedure to be applied, all the weights corresponding to the separate contributions (events and counter events) and the corresponding kinematics, which is in general different between events and each of the counter events, need to be saved in an intermediate event file. With this information it is then possible to recompute the total event weight by reweighting each contribution by the matrix-elements in the FT. The weights corresponding to $\mathcal{B}, \mathcal{V}, \mathcal{C}^{(\rm int)}, \mathcal{C}_{\rm MC}$ are rescaled by the ratio $\mathcal{B}_{\rm FT}/\mathcal{B}_{\rm HEFT}$, while those corresponding to $\mathcal{R}$ by the ratio $\mathcal{R}_{\rm FT}/\mathcal{R}_{\rm HEFT}$. When unweighted events are generated, this amounts into rescaling the whole weight of $\mathbb{S}$-events with Born matrix-elements, and the different terms corresponding to $\mathbb{H}$-events as written above. This solution has the advantage of requiring the FT matrix-elements to be evaluated in significantly fewer phase space points than those used while integrating it directly. In addition, it is completely general and only assumes that there are no regions in phase space where the HEFT gives a vanishing contribution while the full theory does not. In our case this condition is satisfied. Moreover, being non-renormalisable, the HEFT leads to distributions that are in general harder in the high-energy tails than the FT. Therefore using the HEFT to generate

JHEP11(2014)079

events efficiently populates phase space regions that are later suppressed by the FT matrix elements, implying no large degradation of statistical accuracy.

In this work we follow the latter strategy, which we find efficient and general. Such technique has been proposed and employed to include heavy-quark corrections at LO in multi-parton merged samples for single Higgs [82] and HH [43] production. The implementation of the reweighting is simplified considerably by the fact that MadGraph5_aMC@NLO already features the needed structure and automatically stores all the relevant weights (though in a slightly different form than the one presented in eq. (3.1)), in order to evaluate the uncertainties associated with scale variation and PDF on an event-by-event basis as described in [83].

If the two-loop matrix elements were known, our procedure would have allowed to exactly compute cross sections at NLO accuracy and perform event generation at NLO+PS in the FT. As the finite part of the two-loop box virtual correction is unknown, this is not yet possible. In our work, we therefore employ and study the effect of using different approximations for the only unknown terms, while including all one-loop (Born and real) known terms. Once the two-loop results for the virtual corrections become available, it will be possible to include them straightforwardly, for example following the conventions of the Binoth Les Houches Accord [84].

The method described here can be applied to other loop-induced processes, for which suitably defined effective interactions can be used to automatically generate events while the FT one-loop matrix elements can then be employed to correctly reweight the events. As already mentioned, our method has been already used in the NLO calculation of Higgs pair production within the SM in [50] and more recently in the 2HDM in [19]. In this work, we will also apply the same procedure to triple Higgs production. We stress that it could also be applied to other loop-induced processes, such $H + 1$ jet and HZ associated production in gluon-gluon fusion.

4 Higgs pair production

In this section we present the results obtained by applying the method described in the previous section to HH production. The first effects we wish to discuss are those coming from the inclusion of the top-quark width. The relevance of the top-quark width in the context of single Higgs production in gluon-gluon fusion has been discussed in [60] where it has been verified that for a light Higgs below the $t\bar{t}$ threshold the effect is negligible but rises to the percent level for heavier Higgs bosons, i.e., closer to the $t\bar{t}$ threshold. Such virtualities are exactly those relevant for Higgs pair production and one can therefore expect the top-quark width effects not to be negligible.

As already mentioned, in our calculation the $2 \to 2$ and $2 \to 3$ one-loop amplitudes are obtained via MadLoop [56]. The computation is performed using the complex mass scheme for the top quark [85, 86] as implemented in MadLoop and ALOHA in MadGraph5_aMC@NLO. In practice, for the top quark this simply amounts to performing the replacement

$$m_t \to m_t \sqrt{1 - i\Gamma_t/m_t} \tag{4.1}$$

JHEP11(2014)079

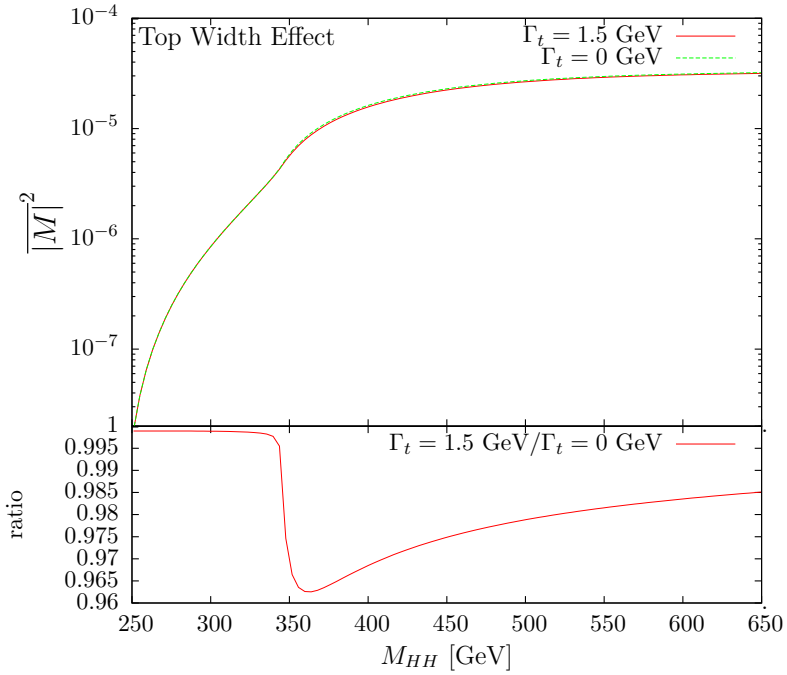

Figure 3. Top width effect on the one-loop (Born) matrix element squared for $gg \to HH$. The results for $\Gamma_t = 0$ and 1.5 GeV are shown along with the corresponding ratio.

everywhere in the computation, i.e. to modify the kinematical mass as well as the Yukawa coupling. The effect of including a non-zero top-quark width is shown in figure 3, where the LO matrix element squared for $gg \to HH$ is plotted as a function of the invariant mass of the Higgs pair for $\Gamma_t = 0$ and 1.5 GeV.[2] A behaviour similar in size and with the same negative sign as the single Higgs case [60] is found, with the non-zero width result displaying a maximum decrease of ∼4% compared to the narrow width result right after the $t\bar{t}$ threshold. The results shown here have been obtained at the matrix element squared level. The final effect on the total cross section at LO at 14 TeV LHC is shown in table 1 and amounts to a correction of ∼-2%. For our NLO predictions we will use a top-quark width of 1.5 GeV.

We now consider the inclusion of the finite top mass in the NLO computation. In what we dub NLO $\text{FT}_{\text{approx}}$, the Born and real configurations are reweighted with the corresponding Born and real emission finite top-quark mass matrix elements and for the virtual configurations, the HEFT result, yet rescaled by the Born in the FT, is used. We stress again that the only approximation made in this procedure is that coming from the absence of the exact results for the two-loop virtual terms. To assess its correctness and study its validity, we have applied the reweighting procedure to single Higgs production in gluon-gluon fusion where all elements of the calculation are available. First, we have validated our procedure using the exact FT real (one-loop) and virtual (two-loop) matrix

[2]We note that here we assumed a 90° scattering for all points included in figure 3, but as the matrix element has an extremely weak angular dependence [25], this provides a perfectly good demonstration of the effect also at the level of the Higgs pair invariant mass distribution.

JHEP11(2014)079

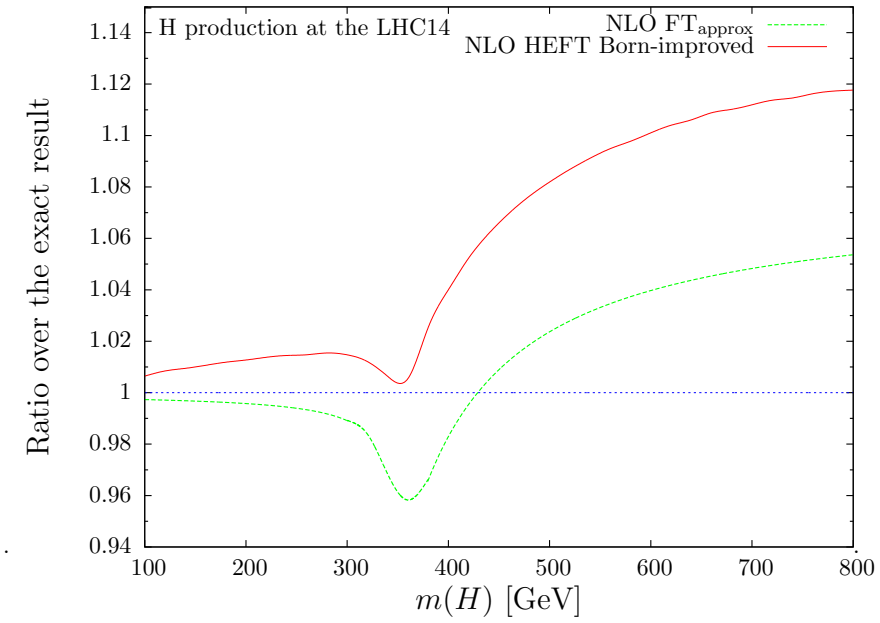

Figure 4. Comparison of the NLO FT$_{\rm approx}$ and HEFT Born-improved results to the exact result for the total cross section for single Higgs production as a function of the Higgs mass.

elements and found excellent agreement with the corresponding exact FT implementations available in MC@NLO v4.0 [87] and SusHi [61]. Second, we have compared two different approximations that can be obtained with our method, the NLO HEFT "Born-improved" ($\sigma^{\rm NLO}_{\rm HEFT} \times \sigma^{\rm LO}_{\rm FT}/\sigma^{\rm LO}_{\rm HEFT}$) and the $FT_{\rm approx}$, to the exact FT results. In figure 4, we show the corresponding ratios to the exact NLO results taken from SusHi [61] at the total cross section level as a function of the Higgs masses. The NLO FT$_{\rm approx}$ remains very close to the exact result for all masses apart from the region in proximity to the $t\bar{t}$ threshold and at very high Higgs mass. In the threshold region a cancellation of the top mass effects between real and virtual corrections takes place, as the Born-improved HEFT result lies very close to the exact one. As it will be important in the following, we note, however, that such a cancellation does not occur above threshold and the FT$_{\rm approx}$ is systematically closer to the exact result than the NLO HEFT Born-improved approximation.

We now consider Higgs pair production and compare the NLO FT$_{\rm approx}$ results to two other approximations. The first of these two approximations corresponds to the "Born-improved" HEFT results. It amounts to rescaling all events, Born and real-emission like, by the Born in the FT, i.e., to always use the weight $\mathcal{B}_{\rm FT}/\mathcal{B}_{\rm HEFT}$. In the case of the real-emission events the kinematics used is that determined by the counter terms mapping. This approach mimics the one used in HPAIR, the only (practically irrelevant) difference being that in HPAIR the reweighting is performed after the integration over the polar angle, while our HEFT Born reweighting is fully differential. Indeed a detailed check with the results of HPAIR shows that once the same parameters are chosen, and in particular the top-width is set to zero, an excellent agreement is found.

JHEP11(2014)079

In addition to the Born-improved HEFT results, we compare our reference results to a second approximation, dubbed NLO $\text{FT}'_{\text{approx}}$, by which we assess the possible shifts of the central value of the NLO cross section due to the inclusion of the exact two-loop corrections in the FT. As already mentioned several times, the two-loop box contributions, e.g., those coming from the second and third diagrams of figure 2 b) are not known. However, the two-loop triangle contributions, e.g., first diagram of figure 2 b), are known (and form a gauge independent subset) as they are the same as those entering single Higgs production. To this aim, we use the finite contribution of the two-loop corrections for single Higgs production, which are publicly available as a function of the Higgs mass, e.g. in SusHi [61], and assume that the same form factor would hold for the two-loop box amplitude. In other words, we proceed under the assumption that these corrections factorise out of the matrix element globally, i.e. for both the box and the triangle diagrams. Needless to say, such an assumption is *ad hoc* and while we do not claim that the triangle form-factor should resemble the box one, this test is still a useful one. The main reason comes from the fact that it allows us to study the extent of possible cancellations taking place between the top-quark mass corrections from the real (which are included) and virtual (which are only approximate) matrix elements. It can be observed[3] that in single Higgs production, where the exact NLO results are available, the "Born-rescaled" HEFT result is extremely close to the exact value for a Higgs mass near the $t\bar{t}$ threshold [88, 89], see figure 4. It is therefore important to assess to which extent such an effect could matter in HH production and impact our NLO $\text{FT}_{\text{approx}}$ predictions as only the exact real emission effects and not those coming from the two-loop virtual contributions are included. As we will argue in the following, the invariant mass region up to the $t\bar{t}$ threshold, i.e. the region where such a cancellation could take place, does not significantly contribute to the Higgs pair production cross section.

We quantify the differences between the approximations discussed above by calculating the total cross section for Higgs pair production in gluon-gluon fusion at 14 TeV in table 1. In this computation, we have set the Higgs mass to $m_H = 125\,\text{GeV}$ and the top-quark mass to $m_t = 172.5\,\text{GeV}$. We note that the top-quark mass dependence of the cross section around the reference top mass of 172.5 GeV can be parametrised approximately (at LO FT as well as at NLO $\text{FT}_{\text{approx}}$) by $\Delta\sigma/\sigma \sim 0.6\% \times \Delta m_t/\text{GeV}$. Parton distribution functions (PDFs) are evaluated by using the MSTW2008 (LO and NLO) parametrisation in the five-flavour scheme [90]. The renormalisation and factorisation scales $\mu_{R,F}$ are set to $\mu_R = \mu_F = \mu_0 = m_{HH}/2$. The dependence of the predictions on scale and PDF variations can be estimated at no extra computational cost via a reweighting technique [83]. Scales are varied independently in the range $\mu_0/2 < \mu_R, \mu_F < 2\mu_0$ and PDF uncertainties at the 68% C.L. are obtained following the prescription given by the MSTW collaboration [90]. Even though b-quark loops can be computed in our setup, b-quark masses as well as their tiny ($\sim$0.3%) contribution to the HH cross section are neglected in the following.

Table 1 collects our results. We first verify that the effect of the non-zero top-quark width on the total cross section at LO, a $\sim 2\%$ decrease, directly follows from the results shown in figure 3 and the fact that the invariant mass distribution peaks at $\sim$400 GeV. We

[3] We are grateful to Michael Spira for bringing up this point.

JHEP11(2014)079

HH production in gluon-gluon fusion at 14 TeV		Cross section [fb]
LO	HEFT	$19.2^{+35.2+2.8\%}_{-24.3-2.9\%}$
	FT, $\Gamma_t = 0\,\text{GeV}$	$23.2^{+32.3+2.0\%}_{-22.9-2.3\%}$
	FT, $\Gamma_t = 1.5\,\text{GeV}$	$22.7^{+32.3+2.0\%}_{-22.9-2.3\%}$
NLO	HEFT	$32.9^{+18.1+2.9\%}_{-15.5-3.7\%}$
	HEFT Born-improved	$38.5^{+18.4+2.0\%}_{-15.1-2.4\%}$
	$\text{FT}_{\text{approx}}$ (virtuals: Born-rescaled HEFT)	$34.3^{+15.0+1.5\%}_{-13.4-2.4\%}$
	$\text{FT}'_{\text{approx}}$ (virtuals: estimated from single Higgs in FT)	$35.0^{+15.7+2.0\%}_{-13.7-2.4\%}$

Table 1. Cross section results (in fb) for Higgs pair production in gluon-gluon fusion at 14 TeV. LO results in the Full Theory are given without and with top-quark width effects. The first NLO result corresponds to the HEFT, while the second to the Born-improved HEFT. The third NLO result, $\text{FT}_{\text{approx}}$, corresponds to our baseline approach where all known top-quark mass corrections coming from one-loop amplitudes are included and the HEFT Born-rescaled approximation for the two-loop amplitudes is used. In the last result, $\text{FT}'_{\text{approx}}$, the information from the known two-loop triangles is also used to estimate the full two-loop contributions. More details are given in the text. All NLO results feature a finite top-quark width. The first uncertainty quoted refers to scale variations, while the second to PDFs. Uncertainties are in percent. No cuts are applied to final state particles and no branching ratios are included.

also note the well-known fact that the process receives large QCD corrections as well as the expected reduction of the theoretical uncertainties for the NLO computations. We then show three NLO results: i) the Born-improved HEFT result through a local event-by-event reweighting, ii) the NLO $\text{FT}_{\text{approx}}$ result, obtained by combining the exact real emission matrix elements, with the Born-rescaled HEFT results for the virtual corrections and iii) the NLO $\text{FT}'_{\text{approx}}$ result obtained by combining the exact real emission matrix elements, with the exact results of single Higgs production for the virtual corrections, as described previously. For all NLO results we keep the finite top-quark width of 1.5 GeV.

We can now compare the different approximations of the FT NLO result. The first important observation is that the Born-improved result is 11% larger than our baseline one. We also note here that the Born-improved result obtained by a local event-by-event rescaling is within 1% of what one would obtain from a global Born rescaling obtained using the total cross section numbers, i.e., $\sigma^{\text{NLO}}_{\text{HEFT}} \times \sigma^{\text{LO}}_{\text{FT}}/\sigma^{\text{LO}}_{\text{HEFT}}$. The difference from the Born-improved result only slightly reduces (9%) when an estimate for the finite top-quark mass terms from the two-loop contributions is included, see last line of table 1. Our NLO $\text{FT}_{\text{approx}}$ result is rather stable in that respect. This is related to the fact that the cancellation we discussed earlier for single Higgs production is only relevant very close to the $t\bar{t}$ threshold, with the Born-rescaled result rapidly rising over the exact one above the threshold. In the case of single Higgs production, we have indeed checked that for Higgs masses above 400 GeV the NLO $\text{FT}_{\text{approx}}$ result (only including the exact real emission matrix element but not the known two-loop virtual results) is closer to the exact result

JHEP11(2014)079

than the corresponding Born-improved one. In the case of Higgs pair production, one could also argue that even if a similar cancellation of the top-quark mass effects between the real and virtual corrections occurred at the $t\bar{t}$ threshold, it would not have a very pronounced effect on the total cross section, as for Higgs pair production the peak of the invariant mass distribution is located at higher mass values.

At this point it is worth to recall the results of ref. [63], where the top-quark mass effects at NLO in QCD were estimated by computing the first few terms in the $1/m_t^2$ expansion for the $K-$factor. The $1/m_t^2$ expansion is known not to converge well at LO [25] and is not supposed to work beyond or even close to the $\sqrt{s} = 2m_t$ threshold, around and beyond which the bulk of the HH cross section resides. However, in ref. [63] an attempt was made by combining the exact Born cross section with the $1/m_t^2$ expanded $K-$factors, as a "taming" technique for the expansion. A +10% increase with respect to the Born-rescaled HEFT result was found, i.e., an effect similar in size but opposite in sign to our estimate. Combined with our findings, the estimate of ref. [63] implies that the difference between the finite part of the Born-rescaled HEFT virtuals and the exact ones should account for a +20% increase of the total cross section, a quite large effect indeed, especially considering that by including top-mass effects in the virtual corrections estimated via the known two-loop triangles, leads only to a couple of percent increase. Besides, we note that the results of the same $1/m_t^2$ expansion approach applied to the production of a single heavy Higgs of mass between 400 and 500 GeV, are known to overestimate the exact results in the FT when no high-energy matching is performed [61, 91–94].

While only an exact calculation of the missing two-loop amplitudes will finally settle this issue, the NLO $\text{FT}_{\text{approx}}$ approach provides central values for the cross sections that appear rather robust, predicting a correction of about -10% with respect to those obtained by means of the Born-improved HEFT. In addition, together with the results of ref. [63], our study provides an estimate of about 10% for the uncertainty to be associated with the HEFT calculation due to the missing top-quark mass effects. Such an uncertainty should be quoted along with the other theoretical uncertainties in the HEFT calculations, at NLO but also at NNLO.

Finally, we note that including the exact one-loop $2 \to 3$ matrix elements provides a more accurate description of the tails of the distributions where hard parton emissions take place, and the factorisation of the $2 \to 3$ real-emission amplitudes into the $2 \to 2$ LO amplitudes, as implicit in the Born-improved approach, cannot accurately describe the hard parton kinematics. To emphasize this point, we compare in figure 5 the differential distributions of the invariant mass and the transverse momentum of the Higgs pair obtained by NLO $\text{FT}_{\text{approx}}$ and Born-improved HEFT. PYTHIA8 [95] has been used for parton shower and hadronisation.

By studying the two distributions, we see that including the exact real emission matrix elements affects the two observables in different ways. On the one hand, for the invariant mass distribution the effect is a uniform modification of the cross section by about 10%. On the other hand, for the transverse momentum of the Higgs pair, at low values where the distribution is dominated by the parton shower, there is no visible difference between the two results, while at high p_T values where the distribution is dominated by hard parton

JHEP11(2014)079

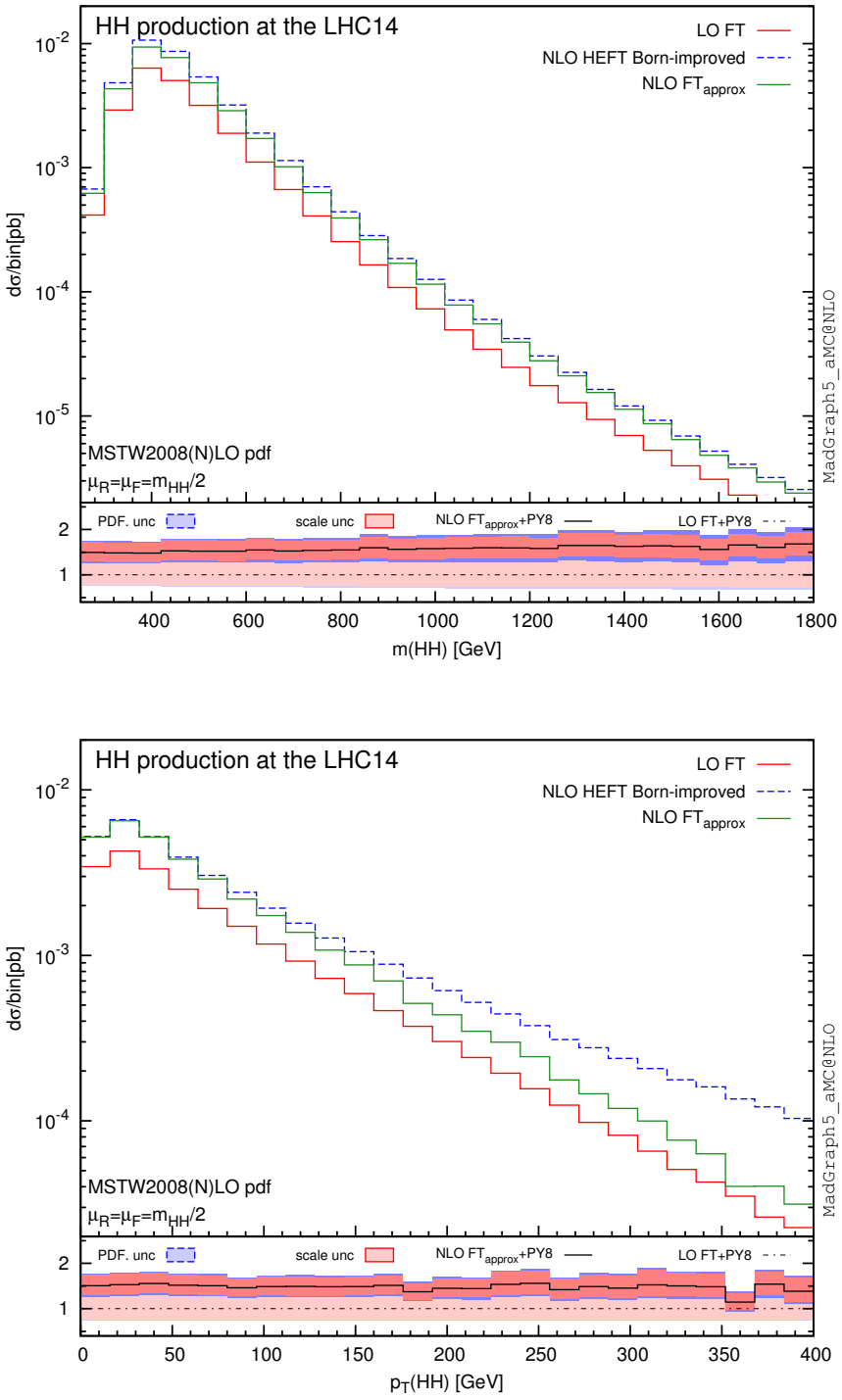

Figure 5. Differential cross sections for the invariant mass and transverse momentum of the Higgs pair in HH production via gluon-gluon fusion at the LHC with 14 TeV centre-of-mass energy. Distributions are obtained by generating events at parton level at LO and NLO accuracy and then matching to PYTHIA8. Uncertainties corresponding to PDF and scale variations are shown in the lower inset.

JHEP11(2014)079

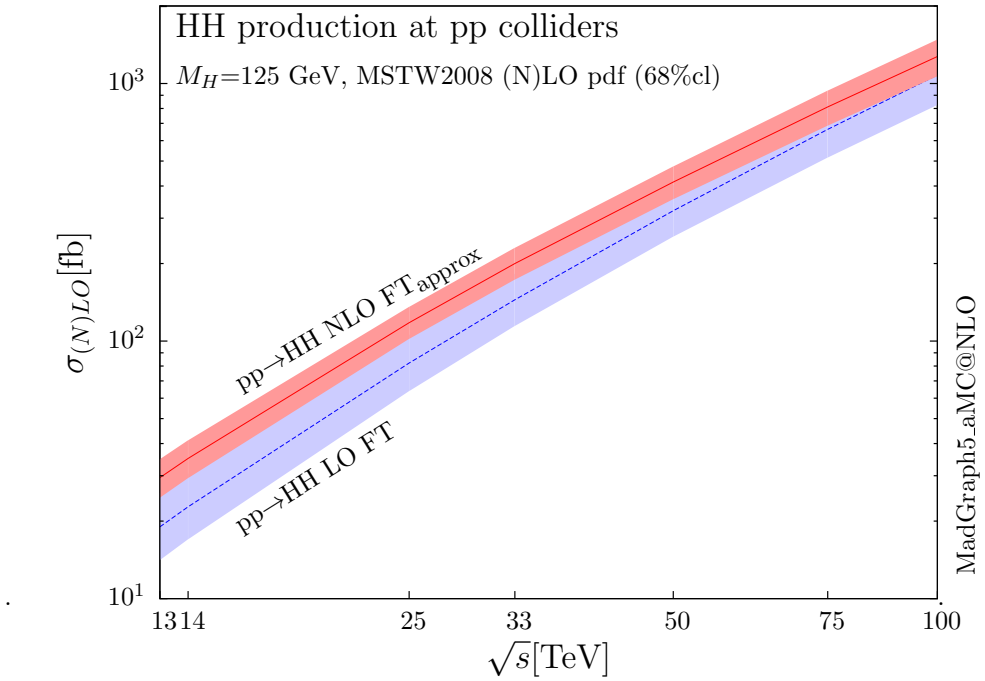

Figure 6. Total cross sections at LO and NLO in QCD in the FT for the Higgs pair production from gluon-gluon fusion at pp colliders as a function of the centre-of-mass energy. The thickness of the lines corresponds to the scale variation and PDF uncertainties added linearly.

$\sigma(HH)$ [fb]	$\sqrt{s} = 14\,\text{TeV}$	$\sqrt{s} = 33\,\text{TeV}$	$\sqrt{s} = 100\,\text{TeV}$
LO FT	$22.7\ ^{+32.3+2.0\%}_{-22.9-2.3\%}$	$145\ ^{+24.9+1.2\%}_{+18.9-1.9\%}$	$1080\ ^{+28.6+1.0\%}_{-21.8-1.7\%}$
NLO FT$_{\text{approx}}$	$34.3^{+15.0+1.5\%}_{-13.4-2.4\%}$	$199\ ^{+13.2+1.3\%}_{-11.6-1.6\%}$	$1250\ ^{+14.8+1.0\%}_{-14.4-1.6\%}$

Table 2. LO and NLO total cross sections (in fb) for Higgs pair production in gluon-gluon fusion at $\sqrt{s} = 14, 33, 100\,\text{TeV}$ in the FT. The uncertainties (in percent) refer to scale variations and to PDF, respectively. No cuts are applied to final state particles and no branching ratios are included.

emission, coming from the real matrix elements, we see that there is a significant deviation from the Born-improved result. In that region we trust our FT$_{\text{approx}}$ prediction more as it describes better the kinematics.

For completeness, we also show the results for the total cross section at LO and NLO for Higgs pair production in gluon-gluon fusion as a function of the hadronic centre-of-mass energy in figure 6, including the uncertainties due to scale variation and PDF added linearly. The uncertainty bands demonstrate nicely the reduction of the scale uncertainties for the NLO calculation. Results for a selected number of hadronic energies are also shown in table 2.

JHEP11(2014)079

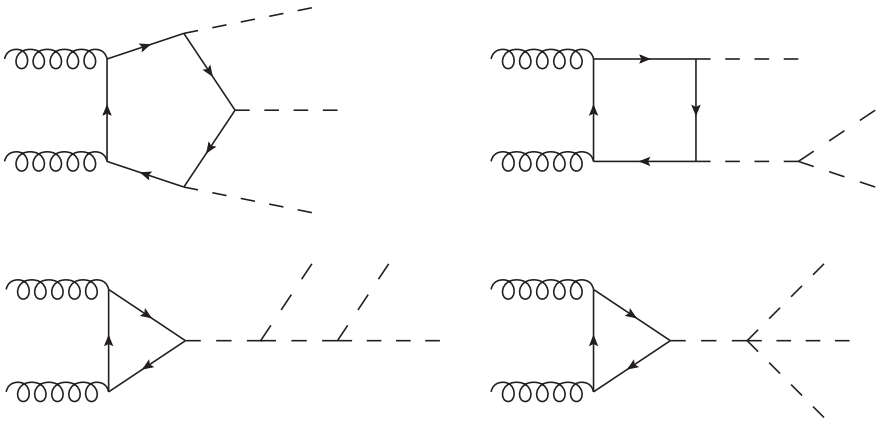

Figure 7. Representative Feynman diagrams for triple Higgs production in gluon-gluon fusion.

5 Higgs triple production

We now apply the same procedure followed for Higgs pair production to obtain results beyond the LO for triple Higgs production through gluon-gluon fusion. Representative topologies of diagrams that contribute to the process at LO are shown in figure 7. These include pentagons where the Higgs bosons couple only to the heavy quarks of the loop, boxes in combination with one power of the trilinear Higgs coupling and triangles with either two powers of the trilinear coupling or the quartic Higgs coupling. It turns out that at LO, the hierarchy of the various contributions in decreasing size order is first pentagons, then boxes and finally triangles [13]. With the triangles contribution already being the smallest of the three, and the fact that the quartic coupling itself has only a very small contribution to that (it only appears in one of the four diagrams), any attempt to access the quartic coupling through the measurement of this process becomes not feasible at the LHC and extremely challenging even at a future 100 TeV collider. In any case, measuring the quartic Higgs coupling in this process would require a very precise knowledge of the triple Higgs coupling [13]. The situation could possibly change in the presence of physics beyond the SM. In this respect having predictions as accurate as possible for production cross sections at hadron colliders in the SM is still be very useful.

We therefore propose to follow the same procedure as for Higgs pair production and improve the NLO HEFT results by systematically including the information from the FT one-loop amplitudes, the Born and the real contributions. In this case, the information which will be included in an approximated way is that related to the two-loop boxes and two-loop pentagons, whose calculation is extremely challenging (note that even the two-loop boxes are more complicated than those in HH production as they feature one more scale) and probably will not be available for some time. The method and the setup follows exactly that of HH, even though the calculation is more complicated and the resulting reweighting procedure is substantially slower. For this process, we find it necessary to use a small computing cluster and fully parallelise the reweighting on an event-by-event basis.

JHEP11(2014)079

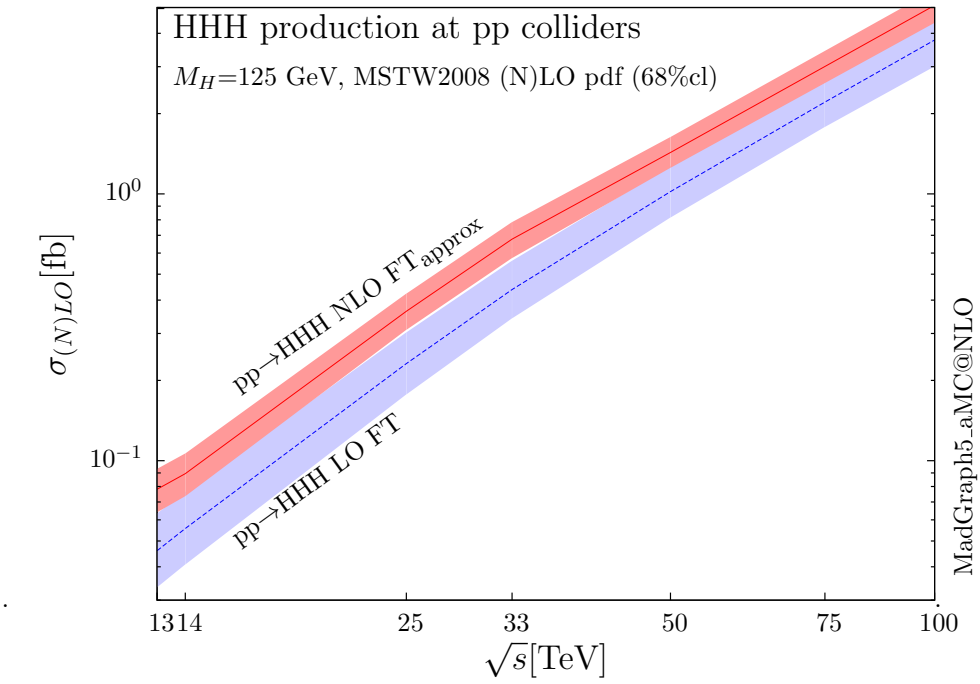

Figure 8. Total cross sections at LO and NLO in QCD in the FT for the triple Higgs production from gluon-gluon fusion at *pp* colliders as a function of the centre-of-mass energy. The thickness of the lines corresponds to the scale and PDF uncertainties added linearly.

$\sigma(HHH)$ [fb]	$\sqrt{s} = 14\,\text{TeV}$	$\sqrt{s} = 33\,\text{TeV}$	$\sqrt{s} = 100\,\text{TeV}$
LO FT	$0.0557\ ^{+34.5+2.5\%}_{-24.0-2.7\%}$	$0.438\ ^{+26.8+1.5\%}_{+20.0-2.0\%}$	$3.78\ ^{+24.1+0.9\%}_{-18.7-1.7\%}$
NLO FT$_{\text{approx}}$	$0.0894^{+16.5+2.5\%}_{-14.6-3.2\%}$	$0.677\ ^{+14.5+1.4\%}_{-13.4-1.7\%}$	$5.09\ ^{+13.5+1.0\%}_{-12.7-1.3\%}$

Table 3. LO and NLO total cross sections (in fb) for triple Higgs production in gluon-gluon fusion at $\sqrt{s} = 14, 33, 100\,\text{TeV}$ in the FT. The uncertainties (in percent) refer to scale variations and to PDF, respectively. No cuts are applied to final state particles and no branching ratios are included.

We show our results for the production cross sections as a function of the centre-of-mass energy in figure 8 and a few representative results in table 3. The NLO calculation leads to $K-$factors and uncertainties which are similar to Higgs pair production. The most important information conveyed by figure 8 is that the cross section remains very small even at 100 TeV *pp* collisions.

We conclude by showing the NLO+PS effects in two key distributions, i.e. that of the invariant mass of the three Higgs-bosons and the transverse momentum of the triplet in figure 9. The latter distribution features two important damping effects: at small $p_T(HHH)$ the spectrum is softened by the soft resummation performed by the shower and at high $p_T(HHH)$ where the top-quark loop effects matter and the HEFT is not reliable.

JHEP11(2014)079

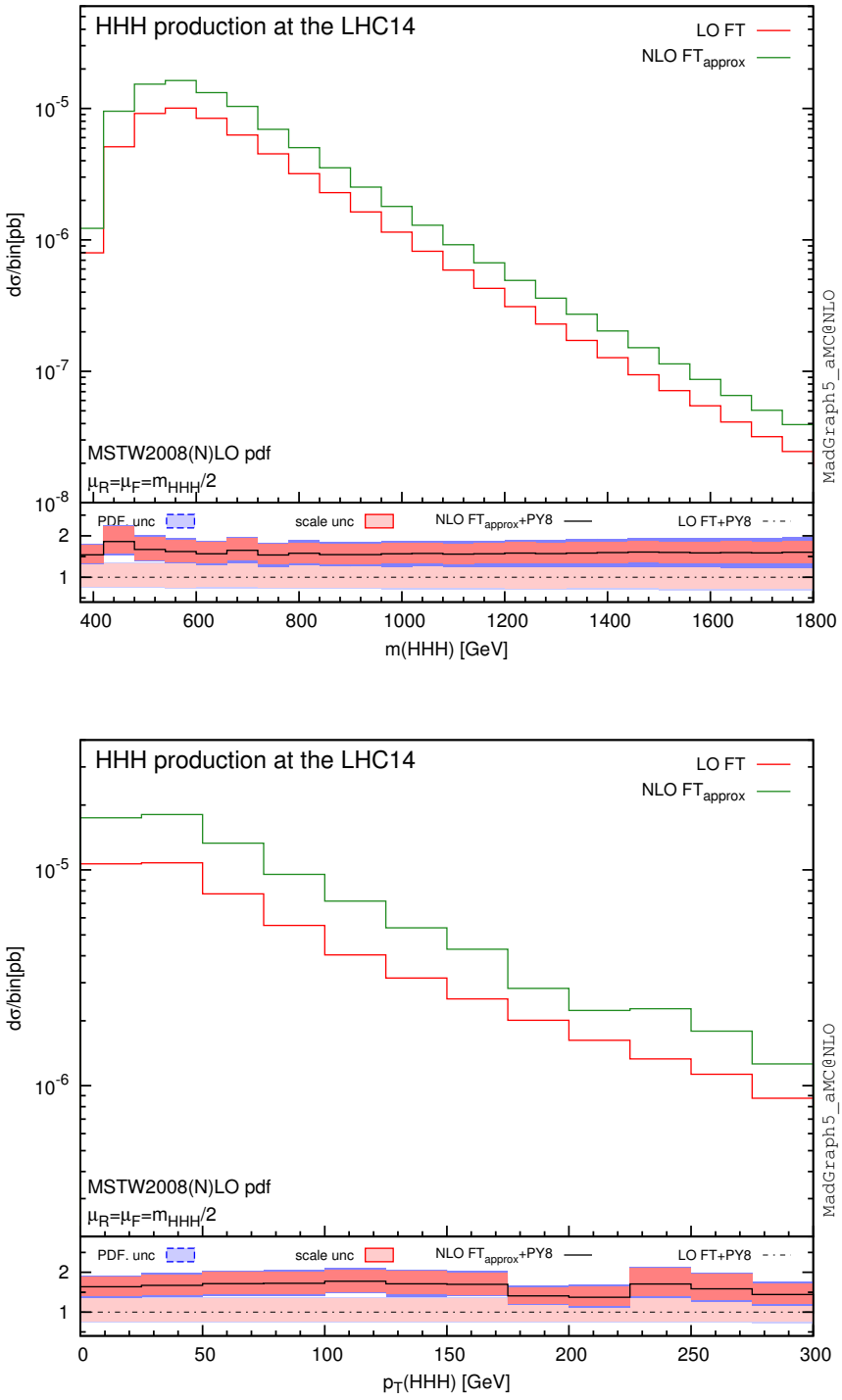

Figure 9. Differential cross sections for the invariant mass and transverse momentum of the three Higgs system in HHH production via gluon-gluon fusion at the LHC with 14 TeV centre-of-mass energy. Distributions are obtained by generating events at parton level at LO and NLO accuracy and then matching to PYTHIA8. Uncertainties corresponding to PDF and scale variations are shown in the lower inset.

JHEP11(2014)079

6 Conclusions

The observation of multiple Higgs production at hadron colliders is a very challenging task, yet a crucial one to obtain key information on the form of the Higgs potential. Rates for these processes are rather low and the accessible signatures swamped by large backgrounds. In any case, any effort to gather information from measurements or bounds on these processes requires accurate predictions for the SM total cross sections. In addition, differential distributions are needed not only to calculate acceptances but also to improve the potential of disentangling these processes from the various backgrounds by selecting the most sensitive regions in phase space. As in single Higgs production, the largest rates for multiple Higgs production come from gluon-gluon fusion mediated by a top-quark loop. Loop-induced processes pose one with the difficulty of obtaining higher order predictions, as these require the computation of multi-loop Feynman diagrams.

In this work we have first focused on Higgs pair production by considering different approximations to improve the HEFT NLO calculation upon the infinite top-quark mass limit. We have introduced a reweighting procedure that allows the inclusion of the top-quark mass and width effects exactly. We have then applied it to HH production using the available information, i.e. the exact (Born and real) one-loop amplitudes and the approximated two-loop matrix elements to appropriately reweight events generated automatically by means of the MC@NLO method in the effective field theory. As a first result and at variance with single Higgs production, we have found that including a non-zero top-quark width reduces the cross section by a couple of percents, the largest effect reaching -4% just above the $t\bar{t}$ threshold.

We have then performed a study to assess the relevance of various corrections and the accuracy of other approaches used in the literature to approximate NLO results in the FT. In particular we have compared to a Born reweighting, where only the exact Born results are used to improve upon the HEFT results. At the total cross section level our best estimate gives a result about 10% smaller than the Born-improved HEFT. We have then considered the difference between the two approaches for differential distributions, and found that including the exact real emission matrix elements provides a better description of the phase space regions where hard emissions take place. We have then argued that total rates are improved too: by using an estimated form of the unknown virtual corrections in the FT using available results from single Higgs production, we have shown that our results are rather stable under variations of the unknown finite terms. Even though the effect of the missing two-loop virtual corrections on the total cross section cannot be quantified until these become available, comparing the different approximations allows one to conservatively associate an uncertainty of order 10% with the calculation due to the missing top-quark mass effects. Note that this uncertainty should be quoted along with others until the exact NLO result becomes available. Finally, we have applied our method to triple Higgs production, providing for the first time predictions for hadron colliders at NLO (+PS) accuracy in the SM. We have found a reduction of the theoretical uncertainties and enhancements of the cross section similar to those of HH production over a large range of collision energies.

JHEP11(2014)079

Acknowledgments

We are grateful to Claude Duhr, Giampiero Passarino, and Michael Spira for stimulating discussions, and to Marius Wiesemann, Tobias Neumann and Michael Rauch for their collaboration. We thank Stefano Frixione for many discussions and for comments on the manuscript. This work has been supported in part by the Research Executive Agency (REA) of the European Union under the Grant Agreement number PITN-GA-2010-264564 (LHCPhenoNet) and PITN-GA-2012-315877 (MCNet). The work of MZ is partially supported by the ILP LABEX (ANR- 10-LABX-63), in turn supported by French state funds managed by the ANR within the "Investissements d'Avenir" programme under reference ANR-11-IDEX-0004-02.

References

[1] F. Englert and R. Brout, *Broken Symmetry and the Mass of Gauge Vector Mesons*, *Phys. Rev. Lett.* **13** (1964) 321 [INSPIRE].

[2] P.W. Higgs, *Broken Symmetries and the Masses of Gauge Bosons*, *Phys. Rev. Lett.* **13** (1964) 508 [INSPIRE].

[3] S. Weinberg, *Implications of Dynamical Symmetry Breaking*, *Phys. Rev.* **D 13** (1976) 974 [INSPIRE].

[4] CMS collaboration, *Evidence for a particle decaying to W^+W^- in the fully leptonic final state in a standard model Higgs boson search in pp collisions at the LHC*, CMS-PAS-HIG-13-003 (2013).

[5] CMS collaboration, *Evidence for the 125 GeV Higgs boson decaying to a pair of τ leptons*, CMS-HIG-13-004 (2014).

[6] CMS collaboration, *Search for a Higgs boson decaying into a Z and a photon in pp collisions at $\sqrt{s} = 7$ and 8 TeV*, CMS-HIG-13-006 (2013).

[7] CMS collaboration, *Search for SM Higgs in WH to WWW to 3l 3nu*, CMS-HIG-13-009 (2013).

[8] ATLAS collaboration, *Search for the Standard Model Higgs boson in the $H \to Z\gamma$ decay mode with pp collisions at $\sqrt{s} = 7$ and 8 TeV*, ATLAS-CONF-2013-009 (2013).

[9] ATLAS collaboration, *Search for a Standard Model Higgs boson in $H \to \mu\mu$ decays with the ATLAS detector*, ATLAS-CONF-2013-010 (2013).

[10] ATLAS collaboration, *Measurements of the properties of the Higgs-like boson in the two photon decay channel with the ATLAS detector using 25 fb^{-1} of proton-proton collision data*, ATLAS-CONF-2013-012 (2013).

[11] ATLAS collaboration, *Measurements of the properties of the Higgs-like boson in the four lepton decay channel with the ATLAS detector using 25 fb^{-1} of proton-proton collision data*, ATLAS-CONF-2013-013 (2013).

JHEP11(2014)079

[12] T. Plehn, M. Spira and P.M. Zerwas, *Pair production of neutral Higgs particles in gluon-gluon collisions*, *Nucl. Phys.* **B 479** (1996) 46 [*Erratum ibid.* **B 531** (1998) 655] [hep-ph/9603205] [INSPIRE].

[13] T. Plehn and M. Rauch, *The quartic Higgs coupling at hadron colliders*, *Phys. Rev.* **D 72** (2005) 053008 [hep-ph/0507321] [INSPIRE].

[14] U. Baur, T. Plehn and D.L. Rainwater, *Measuring the Higgs boson self coupling at the LHC and finite top mass matrix elements*, *Phys. Rev. Lett.* **89** (2002) 151801 [hep-ph/0206024] [INSPIRE].

[15] U. Baur, T. Plehn and D.L. Rainwater, *Examining the Higgs boson potential at lepton and hadron colliders: A Comparative analysis*, *Phys. Rev.* **D 68** (2003) 033001 [hep-ph/0304015] [INSPIRE].

[16] U. Baur, T. Plehn and D.L. Rainwater, *Probing the Higgs selfcoupling at hadron colliders using rare decays*, *Phys. Rev.* **D 69** (2004) 053004 [hep-ph/0310056] [INSPIRE].

[17] T. Binoth, S. Karg, N. Kauer and R. Ruckl, *Multi-Higgs boson production in the Standard Model and beyond*, *Phys. Rev.* **D 74** (2006) 113008 [hep-ph/0608057] [INSPIRE].

[18] J. Baglio, O. Eberhardt, U. Nierste and M. Wiebusch, *Benchmarks for Higgs Pair Production and Heavy Higgs Searches in the Two-Higgs-Doublet Model of Type II*, *Phys. Rev.* **D 90** (2014) 015008 [arXiv:1403.1264] [INSPIRE].

[19] B. Hespel, D. Lopez-Val and E. Vryonidou, *Higgs pair production via gluon fusion in the Two-Higgs-Doublet Model*, *JHEP* **09** (2014) 124 [arXiv:1407.0281] [INSPIRE].

[20] E. Asakawa, D. Harada, S. Kanemura, Y. Okada and K. Tsumura, *Higgs boson pair production in new physics models at hadron, lepton and photon colliders*, *Phys. Rev.* **D 82** (2010) 115002 [arXiv:1009.4670] [INSPIRE].

[21] A. Arhrib, R. Benbrik, C.-H. Chen, R. Guedes and R. Santos, *Double Neutral Higgs production in the Two-Higgs doublet model at the LHC*, *JHEP* **08** (2009) 035 [arXiv:0906.0387] [INSPIRE].

[22] J. Cao, Z. Heng, L. Shang, P. Wan and J.M. Yang, *Pair Production of a 125 GeV Higgs Boson in MSSM and NMSSM at the LHC*, *JHEP* **04** (2013) 134 [arXiv:1301.6437] [INSPIRE].

[23] U. Ellwanger, *Higgs pair production in the NMSSM at the LHC*, *JHEP* **08** (2013) 077 [arXiv:1306.5541] [INSPIRE].

[24] D.T. Nhung, M. Muhlleitner, J. Streicher and K. Walz, *Higher Order Corrections to the Trilinear Higgs Self-Couplings in the Real NMSSM*, *JHEP* **11** (2013) 181 [arXiv:1306.3926] [INSPIRE].

[25] S. Dawson, E. Furlan and I. Lewis, *Unravelling an extended quark sector through multiple Higgs production?*, *Phys. Rev.* **D 87** (2013) 014007 [arXiv:1210.6663] [INSPIRE].

[26] G.D. Kribs and A. Martin, *Enhanced di-Higgs Production through Light Colored Scalars*, *Phys. Rev.* **D 86** (2012) 095023 [arXiv:1207.4496] [INSPIRE].

[27] C.-Y. Chen, S. Dawson and I.M. Lewis, *Top Partners and Higgs Boson Production*, *Phys. Rev.* **D 90** (2014) 035016 [arXiv:1406.3349] [INSPIRE].

JHEP11(2014)079

[28] C.O. Dib, R. Rosenfeld and A. Zerwekh, *Double Higgs production and quadratic divergence cancellation in little Higgs models with T parity*, *JHEP* **05** (2006) 074 [hep-ph/0509179] [INSPIRE].

[29] L. Wang, W. Wang, J.M. Yang and H. Zhang, *Higgs-pair production in littlest Higgs model with T-parity*, *Phys. Rev.* **D 76** (2007) 017702 [arXiv:0705.3392] [INSPIRE].

[30] M.J. Dolan, C. Englert and M. Spannowsky, *New Physics in LHC Higgs boson pair production*, *Phys. Rev.* **D 87** (2013) 055002 [arXiv:1210.8166] [INSPIRE].

[31] J.M. No and M. Ramsey-Musolf, *Probing the Higgs Portal at the LHC Through Resonant di-Higgs Production*, *Phys. Rev.* **D 89** (2014) 095031 [arXiv:1310.6035] [INSPIRE].

[32] E.L. Berger, S.B. Giddings, H. Wang and H. Zhang, *Higgs-flavon mixing and LHC phenomenology in a simplified model of broken flavor symmetry*, *Phys. Rev.* **D 90** (2014) 076004 [arXiv:1406.6054] [INSPIRE].

[33] R. Grober and M. Muhlleitner, *Composite Higgs Boson Pair Production at the LHC*, *JHEP* **06** (2011) 020 [arXiv:1012.1562] [INSPIRE].

[34] M. Gillioz, R. Grober, C. Grojean, M. Muhlleitner and E. Salvioni, *Higgs Low-Energy Theorem (and its corrections) in Composite Models*, *JHEP* **10** (2012) 004 [arXiv:1206.7120] [INSPIRE].

[35] R. Contino et al., *Anomalous Couplings in Double Higgs Production*, *JHEP* **08** (2012) 154 [arXiv:1205.5444] [INSPIRE].

[36] A. Pierce, J. Thaler and L.-T. Wang, *Disentangling Dimension Six Operators through Di-Higgs Boson Production*, *JHEP* **05** (2007) 070 [hep-ph/0609049] [INSPIRE].

[37] J. Liu, X.-P. Wang and S.-h. Zhu, *Discovering extra Higgs boson via pair production of the SM-like Higgs bosons*, arXiv:1310.3634 [INSPIRE].

[38] A. Papaefstathiou, L.L. Yang and J. Zurita, *Higgs boson pair production at the LHC in the $b\bar{b}W^+W^-$ channel*, *Phys. Rev.* **D 87** (2013) 011301 [arXiv:1209.1489] [INSPIRE].

[39] J. Baglio et al., *The measurement of the Higgs self-coupling at the LHC: theoretical status*, *JHEP* **04** (2013) 151 [arXiv:1212.5581] [INSPIRE].

[40] M.J. Dolan, C. Englert and M. Spannowsky, *Higgs self-coupling measurements at the LHC*, *JHEP* **10** (2012) 112 [arXiv:1206.5001] [INSPIRE].

[41] A.J. Barr, M.J. Dolan, C. Englert and M. Spannowsky, *Di-Higgs final states augMT2ed – selecting hh events at the high luminosity LHC*, *Phys. Lett.* **B 728** (2014) 308 [arXiv:1309.6318] [INSPIRE].

[42] M. Gouzevitch et al., *Scale-invariant resonance tagging in multijet events and new physics in Higgs pair production*, *JHEP* **07** (2013) 148 [arXiv:1303.6636] [INSPIRE].

[43] Q. Li, Q.-S. Yan and X. Zhao, *Higgs Pair Production: Improved Description by Matrix Element Matching*, *Phys. Rev.* **D 89** (2014) 033015 [arXiv:1312.3830] [INSPIRE].

[44] F. Goertz, A. Papaefstathiou, L.L. Yang and J. Zurita, *Higgs Boson self-coupling measurements using ratios of cross sections*, *JHEP* **06** (2013) 016 [arXiv:1301.3492] [INSPIRE].

[45] D.E. Ferreira de Lima, A. Papaefstathiou and M. Spannowsky, *Standard model Higgs boson pair production in the $(b\bar{b})(b\bar{b})$ final state*, *JHEP* **08** (2014) 030 [arXiv:1404.7139] [INSPIRE].

JHEP11(2014)079

[46] V. Barger, L.L. Everett, C.B. Jackson and G. Shaughnessy, *Higgs-Pair Production and Measurement of the Triscalar Coupling at LHC(8,14)*, *Phys. Lett.* **B 728** (2014) 433 [arXiv:1311.2931] [INSPIRE].

[47] M. Slawinska, W. van den Wollenberg, B. van Eijk and S. Bentvelsen, *Phenomenology of the trilinear Higgs coupling at proton-proton colliders*, arXiv:1408.5010 [INSPIRE].

[48] R. Contino, C. Grojean, D. Pappadopulo, R. Rattazzi and A. Thamm, *Strong Higgs Interactions at a Linear Collider*, *JHEP* **02** (2014) 006 [arXiv:1309.7038] [INSPIRE].

[49] D. Pappadopulo, A. Thamm, R. Torre and A. Wulzer, *Heavy Vector Triplets: Bridging Theory and Data*, *JHEP* **09** (2014) 060 [arXiv:1402.4431] [INSPIRE].

[50] R. Frederix et al., *Higgs pair production at the LHC with NLO and parton-shower effects*, *Phys. Lett.* **B 732** (2014) 142 [arXiv:1401.7340] [INSPIRE].

[51] L. Liu-Sheng et al., *NNLO QCD corrections to Higgs pair production via vector boson fusion at hadron colliders*, *Phys. Rev.* **D 89** (2014) 073001 [arXiv:1401.7754] [INSPIRE].

[52] S. Dawson, S. Dittmaier and M. Spira, *Neutral Higgs boson pair production at hadron colliders: QCD corrections*, *Phys. Rev.* **D 58** (1998) 115012 [hep-ph/9805244] [INSPIRE].

[53] D. de Florian and J. Mazzitelli, *Higgs Boson Pair Production at Next-to-Next-to-Leading Order in QCD*, *Phys. Rev. Lett.* **111** (2013) 201801 [arXiv:1309.6594] [INSPIRE].

[54] J. Grigo, K. Melnikov and M. Steinhauser, *Virtual corrections to Higgs boson pair production in the large top quark mass limit*, *Nucl. Phys.* **B 888** (2014) 17 [arXiv:1408.2422] [INSPIRE].

[55] G. Ossola, C.G. Papadopoulos and R. Pittau, *CutTools: A Program implementing the OPP reduction method to compute one-loop amplitudes*, *JHEP* **03** (2008) 042 [arXiv:0711.3596] [INSPIRE].

[56] V. Hirschi et al., *Automation of one-loop QCD corrections*, *JHEP* **05** (2011) 044 [arXiv:1103.0621] [INSPIRE].

[57] D. Graudenz, M. Spira and P.M. Zerwas, *QCD corrections to Higgs boson production at proton proton colliders*, *Phys. Rev. Lett.* **70** (1993) 1372 [INSPIRE].

[58] M. Spira, A. Djouadi, D. Graudenz and P.M. Zerwas, *Higgs boson production at the LHC*, *Nucl. Phys.* **B 453** (1995) 17 [hep-ph/9504378] [INSPIRE].

[59] R. Harlander and P. Kant, *Higgs production and decay: Analytic results at next-to-leading order QCD*, *JHEP* **12** (2005) 015 [hep-ph/0509189] [INSPIRE].

[60] C. Anastasiou, S. Buehler, F. Herzog and A. Lazopoulos, *Total cross-section for Higgs boson hadroproduction with anomalous Standard Model interactions*, *JHEP* **12** (2011) 058 [arXiv:1107.0683] [INSPIRE].

[61] R.V. Harlander, S. Liebler and H. Mantler, *SusHi: A program for the calculation of Higgs production in gluon fusion and bottom-quark annihilation in the Standard Model and the MSSM*, *Computer Physics Communications* **184** (2013) 1605 [arXiv:1212.3249] [INSPIRE].

[62] R.V. Harlander and K.J. Ozeren, *Finite top mass effects for hadronic Higgs production at next-to-next-to-leading order*, *JHEP* **11** (2009) 088 [arXiv:0909.3420] [INSPIRE].

[63] J. Grigo, J. Hoff, K. Melnikov and M. Steinhauser, *On the Higgs boson pair production at the LHC*, *Nucl. Phys.* **B 875** (2013) 1 [arXiv:1305.7340] [INSPIRE].

JHEP11(2014)079

[64] P. Maierhöfer and A. Papaefstathiou, *Higgs Boson pair production merged to one jet*, *JHEP* **03** (2014) 126 [arXiv:1401.0007] [INSPIRE].

[65] D.Y. Shao, C.S. Li, H.T. Li and J. Wang, *Threshold resummation effects in Higgs boson pair production at the LHC*, *JHEP* **07** (2013) 169 [arXiv:1301.1245] [INSPIRE].

[66] J. Alwall et al., *The automated computation of tree-level and next-to-leading order differential cross sections and their matching to parton shower simulations*, *JHEP* **07** (2014) 079 [arXiv:1405.0301] [INSPIRE].

[67] N.D. Christensen and C. Duhr, *FeynRules — Feynman rules made easy*, *Comput. Phys. Commun.* **180** (2009) 1614 [arXiv:0806.4194] [INSPIRE].

[68] A. Alloul, N.D. Christensen, C. Degrande, C. Duhr and B. Fuks, *FeynRules 2.0 — A complete toolbox for tree-level phenomenology*, *Comput. Phys. Commun.* **185** (2014) 2250 [arXiv:1310.1921] [INSPIRE].

[69] P. Artoisenet et al., *A framework for Higgs characterisation*, *JHEP* **11** (2013) 043 [arXiv:1306.6464] [INSPIRE].

[70] A. Alloul, B. Fuks and V. Sanz, *Phenomenology of the Higgs Effective Lagrangian via FEYNRULES*, *JHEP* **04** (2014) 110 [arXiv:1310.5150] [INSPIRE].

[71] F. Maltoni, K. Mawatari and M. Zaro, *Higgs characterisation via vector-boson fusion and associated production: NLO and parton-shower effects*, *Eur. Phys. J.* **74** (2014) 2710 [arXiv:1311.1829] [INSPIRE].

[72] F. Demartin, F. Maltoni, K. Mawatari, B. Page and M. Zaro, *Higgs characterisation at NLO in QCD: CP properties of the top-quark Yukawa interaction*, *Eur. Phys. J.* **C 74** (2014) 3065 [arXiv:1407.5089] [INSPIRE].

[73] G. Ossola, C.G. Papadopoulos and R. Pittau, *Reducing full one-loop amplitudes to scalar integrals at the integrand level*, *Nucl. Phys.* **B 763** (2007) 147 [hep-ph/0609007] [INSPIRE].

[74] C. Degrande, *Automatic evaluation of UV and R2 terms for beyond the Standard Model Lagrangians: a proof-of-principle*, arXiv:1406.3030 [INSPIRE].

[75] B. Page and R. Pittau, *R_2 vertices for the effective ggH theory*, *JHEP* **09** (2013) 078 [arXiv:1307.6142] [INSPIRE].

[76] C. Degrande et al., *UFO — The Universal FeynRules Output*, *Comput. Phys. Commun.* **183** (2012) 1201 [arXiv:1108.2040] [INSPIRE].

[77] P. de Aquino, W. Link, F. Maltoni, O. Mattelaer and T. Stelzer, *ALOHA: Automatic Libraries Of Helicity Amplitudes for Feynman Diagram Computations*, *Comput. Phys. Commun.* **183** (2012) 2254 [arXiv:1108.2041] [INSPIRE].

[78] S. Frixione, Z. Kunszt and A. Signer, *Three jet cross-sections to next-to-leading order*, *Nucl. Phys.* **B 467** (1996) 399 [hep-ph/9512328] [INSPIRE].

[79] S. Catani and M.H. Seymour, *A General algorithm for calculating jet cross-sections in NLO QCD*, *Nucl. Phys.* **B 485** (1997) 291 [*Erratum ibid.* **B 510** (1998) 503] [hep-ph/9605323] [INSPIRE].

[80] S. Frixione and B.R. Webber, *Matching NLO QCD computations and parton shower simulations*, *JHEP* **06** (2002) 029 [hep-ph/0204244] [INSPIRE].

JHEP11(2014)079

[81] R. Frederix, S. Frixione, F. Maltoni and T. Stelzer, *Automation of next-to-leading order computations in QCD: The FKS subtraction*, *JHEP* **10** (2009) 003 [arXiv:0908.4272] [INSPIRE].

[82] J. Alwall, Q. Li and F. Maltoni, *Matched predictions for Higgs production via heavy-quark loops in the SM and beyond*, *Phys. Rev.* **D 85** (2012) 014031 [arXiv:1110.1728] [INSPIRE].

[83] R. Frederix et al., *Four-lepton production at hadron colliders: aMC@NLO predictions with theoretical uncertainties*, *JHEP* **02** (2012) 099 [arXiv:1110.4738] [INSPIRE].

[84] S. Alioli et al., *Update of the Binoth Les Houches Accord for a standard interface between Monte Carlo tools and one-loop programs*, *Comput. Phys. Commun.* **185** (2014) 560 [arXiv:1308.3462] [INSPIRE].

[85] A. Denner, S. Dittmaier, M. Roth and D. Wackeroth, *Predictions for all processes $e^+e^- \to 4$ fermions + γ*, *Nucl. Phys.* **B 560** (1999) 33 [hep-ph/9904472] [INSPIRE].

[86] A. Denner, S. Dittmaier, M. Roth and L.H. Wieders, *Electroweak corrections to charged-current $e^+e^- \to 4$ fermion processes: Technical details and further results*, *Nucl. Phys.* **B 724** (2005) 247 [*Erratum ibid.* **B 854** (2012) 504] [hep-ph/0505042] [INSPIRE].

[87] S. Frixione, F. Stoeckli, P. Torrielli, B.R. Webber and C.D. White, *The MCaNLO 4.0 Event Generator*, arXiv:1010.0819 [INSPIRE].

[88] R. Harlander, *Supersymmetric Higgs production at the Large Hadron Collider*, *Eur. Phys. J.* **C 33** (2004) S454 [hep-ph/0311005] [INSPIRE].

[89] C. Anastasiou, S. Bucherer and Z. Kunszt, *HPro: A NLO Monte-Carlo for Higgs production via gluon fusion with finite heavy quark masses*, *JHEP* **10** (2009) 068 [arXiv:0907.2362] [INSPIRE].

[90] A.D. Martin, W.J. Stirling, R.S. Thorne and G. Watt, *Parton distributions for the LHC*, *Eur. Phys. J.* **C 63** (2009) 189 [arXiv:0901.0002] [INSPIRE].

[91] R.V. Harlander and W.B. Kilgore, *Next-to-next-to-leading order Higgs production at hadron colliders*, *Phys. Rev. Lett.* **88** (2002) 201801 [hep-ph/0201206] [INSPIRE].

[92] R.V. Harlander, T. Neumann, K.J. Ozeren and M. Wiesemann, *Top-mass effects in differential Higgs production through gluon fusion at order α_s^4*, *JHEP* **08** (2012) 139 [arXiv:1206.0157] [INSPIRE].

[93] R.V. Harlander, H. Mantler, S. Marzani and K.J. Ozeren, *Higgs production in gluon fusion at next-to-next-to-leading order QCD for finite top mass*, *Eur. Phys. J.* **C 66** (2010) 359 [arXiv:0912.2104] [INSPIRE].

[94] T. Neumann and M. Wiesemann, *Finite top-mass effects in gluon-induced Higgs production with a jet-veto at NNLO*, arXiv:1408.6836 [INSPIRE].

[95] T. Sjöstrand, S. Mrenna and P.Z. Skands, *A Brief Introduction to PYTHIA 8.1*, *Comput. Phys. Commun.* **178** (2008) 852 [arXiv:0710.3820] [INSPIRE].

JHEP11(2014)079